**Article:**
Derkani, M.H., Bartlett, N.J., Koma, G. et al. (2022) Mechanisms of dispersion of metakaolin particles via adsorption of sodium naphthalene sulfonate formaldehyde polymer. Journal of Colloid and Interface Science, 628 (Part B). pp. 745-757. ISSN: 0021-9797

https://doi.org/10.1016/j.jcis.2022.07.166

Journal of Colloid and Interface Science 628 (2022) 745–757

Contents lists available at ScienceDirect

Journal of Colloid and Interface Science

journal homepage: www.elsevier.com/locate/jcis

# Mechanisms of dispersion of metakaolin particles via adsorption of sodium naphthalene sulfonate formaldehyde polymer

Maryam H. Derkani [a,b,c,*], Nathan J. Bartlett [c], Gaone Koma [b], Laura A. Carter [a], Daniel A. Geddes [a,b], John L. Provis [b], Brant Walkley [a,*]

[a] Department of Chemical and Biological Engineering, University of Sheffield, Sir Robert Hadfield Building, Mappin Street, Sheffield S1 3JD, UK
[b] Department of Materials Science and Engineering, University of Sheffield, Sir Robert Hadfield Building, Mappin Street, Sheffield S1 3JD, UK
[c] Hazelwood Chemical Synthesis, The Lubrizol Corporation, The Knowle, Nether Lane, Hazelwood, Derbyshire DE56 4AN, UK

## GRAPHICAL ABSTRACT

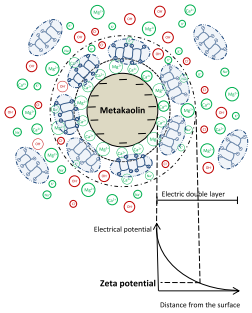


## ARTICLE INFO

*Article history:*
Received 4 May 2022
Revised 20 July 2022
Accepted 26 July 2022
Available online 29 July 2022

*Keywords:*
Calcined clay
Alkali-activated cement
Geopolymer cement
Portland cement
Metakaolin
Sodium naphthalene sulfonate formaldehyde polymer
Zeta potential
Total organic carbon content
Dispersion mechanisms

## ABSTRACT

The influence of different alkali and alkaline earth cations ($Na^+$, $K^+$, $Ca^{2+}$, and $Mg^{2+}$), and of solution pH, on surface interactions of metakaolin particles with a sodium naphthalene sulfonate formaldehyde polymer (SNSFP) (a commercial superplasticizer for concretes) was investigated in aqueous systems relevant to alkali-activated and blended Portland cements. This study used zeta potential measurements, adsorption experiments, and both *in situ* and *ex situ* Fourier transform infrared spectroscopy measurements of the suspensions to gain a fundamental understanding of colloidal interactions and physicochemical mechanisms governing dispersion in this system. SNSFP was most effective in dispersing metakaolin suspensions in $Ca^{2+}$-modified aqueous NaOH systems ($CaCl_2$-NaOH) at dosages of 5 wt.%. Additionally, $Ca^{2+}$ was the most effective alkaline earth cation mediator in providing a dispersion effect in metakaolin dispersed in aqueous NaOH and SNSFP mixtures, while $Mg^{2+}$ was the most effective in aqueous KOH and SNSFP mixtures. The colloidal dispersion remained stable in the highly alkaline environment, and therefore SNSFP could be utilized to improve dispersion of metakaolin-based alkali-activated systems. The suggested mechanism for colloidal stability and fluidity of metakaolin-based cements (e.g. Portland cement blends and alkali-activated cements) is explained by changes in the distribution and structure of the electric double-layer, as well as structural forces, due to alteration in surface charge density and hydrated shell, facilitating competitive adsorption of the polymer.



* Corresponding authors.
*E-mail addresses:* m.derkani@sheffield.ac.uk (M.H. Derkani), nathan.bartlett@lubrizol.com (N.J. Bartlett), j.provis@sheffield.ac.uk (J.L. Provis), b.walkley@sheffield.ac.uk (B. Walkley).

https://doi.org/10.1016/j.jcis.2022.07.166
0021-9797/

## 1. Introduction

Alkali-activated cements have emerged as potentially environmentally sustainable construction materials which can be manufactured from aluminosilicate precursors, including materials with geological origin (e.g. metakaolin) or industrial by-products (e.g. fly ash and ground granulated blast furnace slag), which react with an alkali component (e.g. alkali silicates or hydroxides) via a poly-condensation reaction [1]. The production of alkali-activated cements, including those with lower-calcium binders sometimes called "geopolymers", offers the possibility to reduce the high embodied energy and $CO_2$ emissions attributed to the production of Portland cement (PC) [2,3]. Alkali-activated cements can also be tailored to exhibit strong engineering characteristics which are desirable in the construction industry, namely high compressive strength, good chemical resistance to acid and sulfate attacks, adjustable setting time, and excellent fire resistance [4]. However, the implementation of low-calcium geopolymers, particularly those based on metakaolin as an aluminosilicate source, has mainly been limited to small-scale projects and niche applications. Issues related to workability have been identified as targets for further development in this regard, as some geopolymer formulations are characterized by high apparent viscosity [5].

Commercially available high range water reducing admixtures, also known as superplasticizers, have been extensively developed and designed to improve the fluidity and workability, as well as other properties, of Portland-based cement systems [6]. These surfactant-based admixtures include lignosulfonates (the first generation) and sulfonated naphthalene/melamine formaldehyde (the second generation). The third generation of polymer formulated admixtures consist of polycarboxylate, polyacrylate or polyethylene-based ester or ether copolymers in a comb-like structure [7–9]. Even though these third-generation admixtures have been shown to be highly effective in enhancing rheology and workability of PC, their efficacy in alkali-activated cement systems has been found to be poor [10,11]. This is attributed to their structural instability, insolubility, and degradation in the highly basic media of fresh geopolymers (pH $\geq$ 13), compared to fresh PC (pH $\approx$ 12) [10,11], as well as differing interactions of superplasticizers with various inorganic surfaces, including aluminosilicates in low-calcium geopolymers, compared to those of calcium silicate surfaces in PC. The high level of alkalinity and high electrolyte content of the activator can impede the dispersing effect of the superplasticizer that can be achieved at lower pH values and electrolyte concentrations [12].

Particle surface properties and colloidal interactions control the fluidity and workability of cementitious systems. Colloidal interactions drive the adsorption capacity and interaction of cement particles with different cement admixtures e.g. superplasticizers used to modify rheological properties (viscosity and yield stress) of fresh mixtures. The mechanisms of operation of superplasticizers to attain colloidal stability and dispersion have been shown to be both electrostatic and steric stabilizations in order to disperse the particles and control fluidity [10,11]. Electrostatic repulsion results from the negative charge induced by adsorption of superplasticizers, whereas steric hindrance results from the thickness of the adsorbed layer [13]. The adsorption and efficiency of cement admixtures e.g. superplasticizers depend on pH, ionic type and concentration of the dispersing medium, as well as the surface charge of the particles itself [14]. Zeta potential is an essential parameter to evaluate the electrokinetic properties of solid-liquid and liquid-liquid interfaces, and its magnitude shows the stability of the colloidal system [15,16], indirectly quantifying the adsorption of ions and ionic species on cementitious particles by changes in sign and magnitude of surface electric charges [17,18].

In a recent study, the effect of adsorbed and non-adsorbed amount of polycarboxylate-based superplasticizers on PC particles was investigated using the depletion method [14]. The importance of non-ionic compounds to act as co-dispersants to improve dispersing effect at low water to cement ratios (w/c < 0.3) was discussed. It was suggested that non-polar small molecules can lead to a significant reduction of the surface tension of the pore solution, hence increasing the cement paste fluidity and workability, due to repulsive depletion forces [14]. Therefore, both adsorbing and non-adsorbing portions of the polymer are crucial in improving dispersion and the time dependent fluidity properties (slump-retention), respectively [9,19].

The interactions between polycarboxylate-based superplasticizers and ground granulated blast furnace slag (GGBFS) in synthetic cement pore solution have also been studied using zeta potential and total organic carbon (TOC) measurements [20]. The results indicated that the calcium ($Ca^{2+}$) ions originating from the synthetic cement pore solution and from dissolution of GGBFS act as the charge-determining ions for the slag particles. The adsorption of $Ca^{2+}$ ions on the initially negatively charged slag surfaces in highly alkaline media, and subsequent adsorption of sulfate ions present in synthetic cement pore solution, creates an electric double layer (EDL) consisting of a positively charged Stern layer ($Ca^{2+}$) and a negatively charged diffuse layer ($SO_4^{2-}$). This provides a competitive adsorption between polycarboxylate ether superplasticizers and $SO_4^{2-}$ ions, where highly anionic superplasticizers can desorb $SO_4^{2-}$ ions and adsorb onto the Stern layer, hence creating a strong dispersion effect. Both the anionic charge density of the polymer and the packing density of $Ca^{2+}$ ions adsorbed on the slag surfaces are determining factors in the adsorption of polycarboxylate ethers onto GGBFS, and the resultant efficacy of dispersion. These factors determine the dosage of superplasticizer required to achieve high flowability. Similarly, the effect of $Ca^{2+}$ ions to instigate the adsorption of anionic polycarboxylate-based superplasticizers, and the specific surface area and surface charge of each mineral type present are main factors to consider when designing a superplasticizer mixture to achieve the highest cement flowability, by providing competitive adsorption of cement admixtures [17,21].

Calcined clays (CC), produced by thermal treatment of clay minerals such as kaolinite, present an excellent option as supplementary cementitious materials (SCMs) in Portland-based cements, and as precursors for alkali-activated cements, due to their accessibility in large quantities worldwide, and high reactivity [22]. However, CC are associated with a reduced workability and increased water demand for the cement, due to their specific surface properties and the internal porosity of the individual CC. The particle shape and morphology of CC, including the flat, plate-like or layered particles, play a major role in their low flowability. This highlights the importance of superplasticizers in applications of CC-containing cements to enable potential sustainability advantages to be exploited. In a study by Li et al. [23], the performance of a polycarboxylate ether superplasticizer to disperse metakaolin-rich CC in blended PC was investigated using zeta potential measurements and TOC analysis. Their results indicated that the CC dispersed in a synthetic cement pore solution exhibited highly negative zeta potentials, whilst the surface charge reversed through the uptake of $Ca^{2+}$ from the pore solution, which facilitated adsorption of the superplasticizer. It was concluded that the commercially available polycarboxylate-based superplasticizers can effectively disperse blends of PC and CC, while much higher dosage of superplasticizer is required in order to satisfy the higher water demand [22,23]. Additionally, introducing cationic groups to backbone structure of superplasticizers, as opposed to conventional anionic polymers, can promote interactions with the

surfaces of negatively charged CC minerals [23]. Cationic copolymers where the cationic charge is due to the presence of certain cyclic and/or polycationic groups were used for dispersion of metakaolin-based alkali-activated cement [12]. These cationic copolymers are stable against Hoffmann elimination that occurs at very high pH and their dispersing effect can be further improved by the addition of polyvalent anions [12]. Additionally, in a recent study the stability of metakaolin and related clay particles against pH, total solids concentration, and superplasticiser type and content, was investigated using potentiometric titration, zeta potential, particle size and rheological measurements [24]. It was shown that polycarboxylate-based superplasticizer provided greater stability with critical pH of 7.5 and dispersant content of 0.15%.

Many studies have been conducted to identify the effect of superplasticizers on alkali-activated systems which were synthesized by the reaction of an alkali component with metakaolin [25], slag [10,26–30], fly ash [11,31–36], or blended fly ash and slag [37]. Most of the earlier published studies of superplasticizers with high calcium geopolymers have identified the first generation (lignosulfonate-based) or the second-generation superplasticizers (naphthalene-based) as effective to some degree [26,29,38–40]. In some cases, also the latest generation of superplasticizers (polycarboxylate-based) have been reported also to be effective [37,41]. However, physical instability, including insolubility of superplasticizers in alkaline solutions, as well as chemical instability, due to changes in molecular structure of superplasticizers in the pore solution of alkali-activated systems, are deemed to be two major issues [42,43]. In highly alkaline media, the alkaline hydrolysis of the ester groups yields carboxylate salts and the respective ether, so the steric hindrance of ether chains is diminished and flowability of geopolymers is not enhanced by these admixtures [44]. Similarly, the chemical structures of vinyl copolymer and melamine-based admixtures are altered when exposed to high alkaline media, whereas naphthalene-based admixtures have shown higher stability in very basic environments [8,29]. Additionally, melamine, sodium lignosulfonate and naphthalene-based superplasticizers can also experience instability in silicate activators [43]. However, not all types of superplasticizers undergo structural changes in highly alkaline media and the structural degradation depends on the type and dosage of superplasticizers in addition to the type of binder and activator, as well as the pH of the alkaline solution [8,29,45–47].

A survey of the literature shows that in all cases, the workability (either using flow table spread or slump tests) increased as a result of superplasticizer dose (reported range 1–5 wt.% of binder) [26,29,37–41]. The effect on setting time and compressive and/or flexural strength, however, varies, with both desirable and detrimental effects observed. This has reportedly depended on the type and concentration of the alkali-activator [26,29]. Thus, it appears that the results obtained in each superplasticizer study apply only for that specific AAM mix design [48]. In general, wide variations are evident in the results reported by available literature, due to the variations in the type of activators, admixture properties and reactivity of raw materials [49]. Therefore, it is essential to gain a fundamental understanding of the colloidal interactions and underlying physicochemical mechanisms involved in this complex organic-modified inorganic system, to establish effective interactions between superplasticizers and aluminosilicate precursors in high alkaline media. This will enable improvement of the rheological properties (plasticity and workability) of geopolymers, making them suitable for specific industrial applications as a viable alternative to materials based on PC.

In the present work, surface interactions and adsorption of a commercial naphthalene-based superplasticizer on metakaolin surfaces in aqueous solutions has been studied by adsorption experiments using a TOC analyzer, zeta potential measurements, and attenuated total reflectance Fourier transform infrared (ATR-FTIR) spectroscopy measurements of the dispersions *in situ*, as well as before and after adsorption (*ex situ*). The tests were conducted under a wide range of conditions including varying pH (7–14), ionic type ($Na^+$, $K^+$, $Ca^{2+}$, and $Mg^{2+}$), electrolyte concentration (0–100 mM), and superplasticizer dosage (0–5 wt.%), allowing the effect of different ions and pH on adsorption and colloidal stability of superplasticizers to be determined. The results provide a better understanding of the physicochemical mechanisms at cement-superplasticizer-electrolyte solution interfaces to be established. Such assessment provides further insight into surface interactions between SNSFP and metakaolin particles and determines the optimum superplasticizer dosage, as well as ionic type and concentration in the pore solution required to disperse the particles within a given alkali-activated system. This methodology can be used as a valuable approach to assess colloidal stability, optimum performance and dosage of cement admixtures in non-conventional cementing binder systems, to improve rheological properties of new and more sustainable cements.

## 2. Materials and methods

### 2.1. Materials

MetaMax metakaolin particles were used in this study (BASF and Lawrence Industries, UK). MetaMax metakaolin is produced using a rotary kiln calcination method, and exhibits average particle diameters of 4.49 μm with average dispersity of 0.073 and average count rate of 39.4 kcps (measured in HPLC water by dynamic light scattering with back scatter detection (optical arrangement of 173°) using a Brookhaven ZetaPALS instrument). The particle size distribution data for the metakaolin used in this study, as measured by dynamic light scattering, is presented in Fig. 1.

The chemical composition of the metakaolin as determined by X-ray fluorescence is tabulated in Table 1. The mineralogical composition of the metakaolin measured by X-ray diffraction (XRD) is shown in Fig. 1. XRD data were obtained across a 2θ range of 5°-70° using a Panalytical X'Pert3 Powder X-ray diffractometer with Cu Kα radiation (1.54 Å), a nickel filter, a step size of 0.020° and a count time of 2 s/step. Diffracted background intensity at low angles was reduced using an anti-scatter blade, and an incident beam divergence of 1.0 mm and a 2.5° Soller slit in the diffracted beam were used. Phase identification was performed using Diffrac.EVA V4.1 software with the ICDD PDF4+ 2015 database.

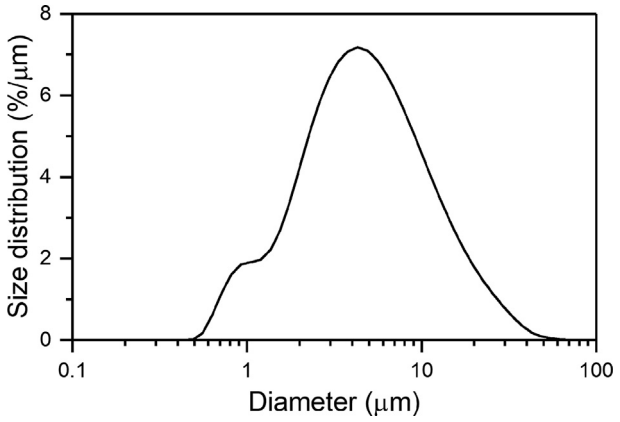


**Fig. 1.** Particle size distribution (PSD) data for the MetaMax metakaolin used in this study.

**Table 1**
Chemical composition data, obtained by X-ray fluorescence (XRF), for the MetaMax metakaolin powder. LOI is loss on ignition at 1000 °C.

| Chemical composition | $SiO_2$ | $Al_2O_3$ | $TiO_2$ | $Fe_2O_3$ | CaO | $K_2O$ | $Na_2O$ | LOI | Others |
|---|---|---|---|---|---|---|---|---|---|
| Weight (%) | 52.54 | 44.54 | 1.31 | 0.36 | <0.05 | 0.15 | 0.21 | 0.63 | 0.2 |

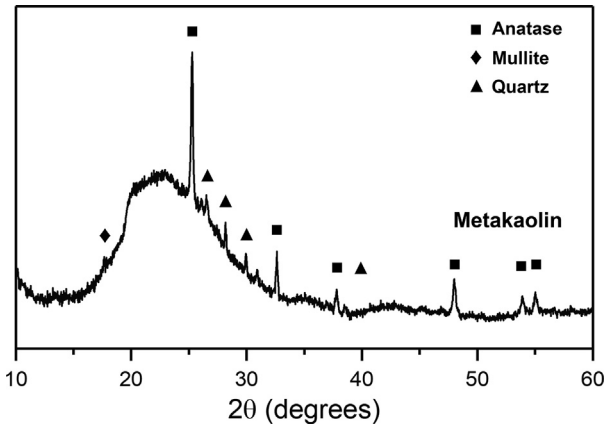


**Fig. 2.** X-ray diffraction (XRD) data for the MetaMax metakaolin used in this study.

The XRD pattern (Fig. 2) displayed a dominant broad feature, due to diffuse scattering, centred at approximately 22° 2θ, consistent with high degree of structural disorder inherent in metakaolin with trace amounts of impurities, including anatase ($TiO_2$, Powder Diffraction File (PDF) # 01-071-1166), quartz ($SiO_2$, PDF # 01-078-1252), and mullite ($Al_6Si_2O_{13}$ (PDF) # 04-012-0161) which are common in commercially sourced metakaolin powder [50].

A commercial superplasticizer, namely sodium naphthalene sulfonate formaldehyde polymer (SNSFP) (Morwet D809) was investigated in this study. Anhydrous calcium chloride (Fisher Scientific, purity ≥ 97 mol. %) and anhydrous magnesium chloride (Sigma Aldrich, purity ≥ 98 mol. %) were used as electrolytes. The pH of the solutions was adjusted using NaOH pellets (Fisher Scientific), KOH pellets (Fisher Scientific) and HPLC grade water (Fisher Scientific).

### 2.2. Experimental design

In order to systematically investigate the surface interactions between metakaolin particles and SNSFP superplasticizer molecules under a wide range of conditions e.g. pH, ionic type and concentration, an experiment was designed to ascertain the optimal conditions for the superplasticizer operation. Fig. 3 below illustrates the design of experiment and sample matrix used in this study. The zeta potential of metakaolin particles was measured as a function of pH (KOH and NaOH) from 7 to 14. This was followed by zeta potential measurements of metakaolin surfaces as function of divalent cationic electrolytes ($CaCl_2$ and $MgCl_2$) at concentrations from 0 to 100 mM, at constant pH. In the next stage, optimum dosage of superplasticizer as the maximum adsorption to the particle surfaces was determined by measuring zeta potential of metakaolin particles as a function superplasticizer dosage (0 to 5 wt.%) at constant pH and electrolyte concentration. Lastly, the stability of the colloidal dispersion was investigated, as a function of pH (11 to 14) at constant superplasticizer dosage and electrolyte concentration.

### 2.3. Sample preparation

Aqueous electrolyte solutions were freshly prepared on the day of experimentation. The pH of the solutions was adjusted using incremental addition of previously prepared NaOH and KOH solutions (1 M) to HPLC water whilst pH was being measured using a SevenExcellence Mettler Toledo pH meter (calibrated before each set of measurements using three buffer solutions with pH of 4.01, 7, and 9.01). The ingress of atmospheric $CO_2$ to the samples was minimized by using sealed containers throughout sample preparation and measurements.

Samples for zeta potential measurements were prepared by adding 0.05 g of metakaolin powder into 50 ml of each electrolyte solution (concentration 1 g/l). Superplasticizer powder was added to the colloidal dispersions, at doses of 1–5 wt.% relative to the mass of metakaolin powder. The suspension was agitated using a roller bed for 1 h to allow equilibrium to be established. Our experimental measurements showed no rapid changes in zeta potential of metakaolin particles over time after 1 h of agitation, indicating that these dispersions are a valid representation of equilibrium conditions.

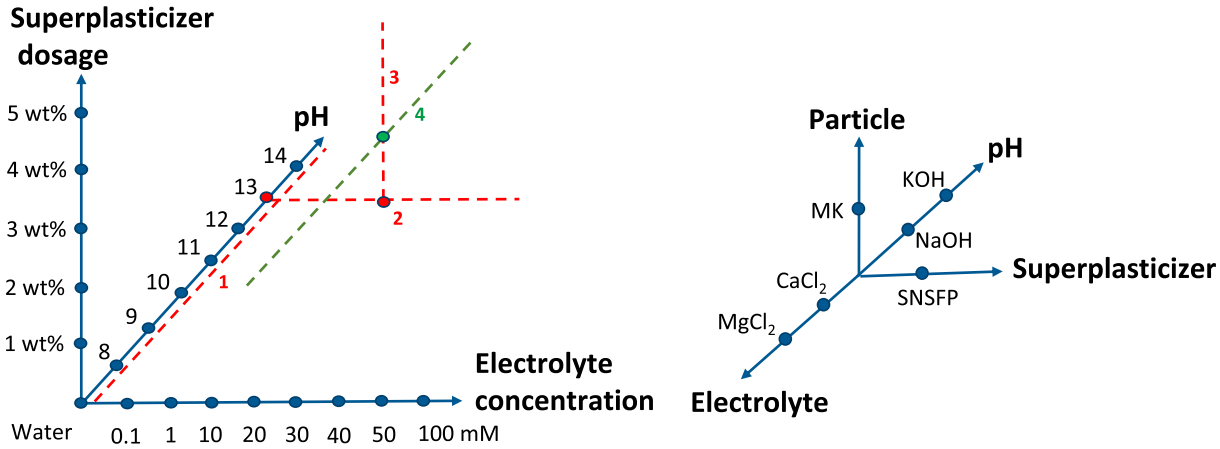


**Fig. 3.** Left: Design of experiments used in this study for defining dosage of superplasticizer at constant pH and constant electrolyte concentration (red-dotted line), and superplasticizer stability as a function of pH at constant dosage of superplasticizer and electrolyte concentration (green-dotted line). Right: Sample matrix illustrating examined particles (MK: metakaolin), superplasticizer (SNSFP: sodium naphthalene sulfonate formaldehyde polymer), pH (NaOH: sodium hydroxide, KOH: potassium hydroxide), and electrolyte type ($CaCl_2$: calcium chloride, $MgCl_2$: magnesium chloride). (For interpretation of the references to colour in this figure legend, the reader is referred to the web version of this article.)

The adsorbed amount of superplasticizer on solid precursors is directly measured using a depletion method by employing a TOC analyzer. This method involves measuring the concentration of superplasticizer present in the mixing water before coming into contact with the cementitious surfaces and comparing this to the non-adsorbed portion of superplasticizer remaining in the solution after mixing [17,18]. The difference in concentration before and after contact with the solid precursor is owed to the adsorption of the superplasticizers on the mineral surfaces. Samples for TOC content measurements were prepared following that of the zeta potential measurements. Two control samples were also prepared, one with all the components of the suspensions except metakaolin (positive control) and the other with all the components except superplasticizer (negative control). After 1 h in the roller bed to allow adsorption, the samples were then filtered under vacuum using a 2.7 μm pore size filter paper. The filtrates were analyzed via TOC content measurements from which adsorption isotherms could be derived, while the filtered powders after adsorption (ex situ) were analyzed via ATR-FTIR spectroscopy measurements. Samples for liquid phase ATR-FTIR spectroscopy measurements of the dispersions *in situ* were prepared following that of zeta potential measurements.

### 2.4. Zeta potential

Zeta potential measurements of metakaolin particles in aqueous electrolyte solutions were performed by phase analysis light scattering (PALS) using a Brookhaven ZetaPALS instrument in a closed system (AQ-752 electrode) with a sinusoidally varying electric field [51]. The PALS method was selected due to its suitability for samples with low mobility, including high salt concentration [52].

Zeta potential measurements of metakaolin samples were performed at 25 °C and ambient pressure. The measurement on each sample was repeated 5 times (consisting of 30 runs), and mean values with standard errors are reported. Measurements were repeated using additionally prepared samples to ensure consistency of results. Disposable plastic cuvettes (ratiolab™ Macro Q-VETTES – Fisher scientific) were used for single sequences of measurements for each sample from low to high pH or concentration, to reduce the risk of cross contamination.

### 2.5. Total organic carbon content

TOC data were acquired by combustion over an oxidation catalyst at 680 °C using a Shimadzu TOC-L CPH/CPN Analyzer with an NDIR detector and 150 ml/min zero grade air as the carrier gas. The adsorbed amount of SNSFP was calculated from the difference between the TOC content of the control solutions and the colloidal dispersion, including both metakaolin and superplasticizer for each sample.

### 2.6. Fourier transform infrared spectroscopy

Attenuated total reflectance Fourier Transform infrared spectroscopy (ATR-FTIR) data for the colloidal dispersions (liquid phase) and the powders (solid-phase) were measured in the range of 500 to 4000 $cm^{-1}$ using a Thermo Fisher Nicolet iS5 FTIR spectrometer equipped with a Specac Golden Gate Single Reflection Diamond ATR System, KBr optics, a diamond ATR crystal, and ZnSe lenses. Each spectrum was the average of 64 scans with a spectral resolution of 2 $cm^{-1}$. Data for each colloidal dispersion (liquid phase) were collected *in situ* by placing a drop of the dispersion on the ATR diamond, and using a cap to block light passing though the samples during measurements.

## 3. Results and discussion

### 3.1. Zeta potential

#### 3.1.1. Effect of pH

Zeta potential values of metakaolin surfaces were measured as a function of hydroxide ($OH^-$) ion concentration from $[OH^-] = 10^{-7}$ M (pH 7) to $[OH^-]$ = 1 M (pH 14) to examine the effect of pH and alkali cations e.g. $Na^+$ and $K^+$ on surface interactions and stability of the metakaolin particle dispersions, Fig. 4. The metakaolin particles exhibit strong negative surface charges in water (pH 7) with a zeta potential of −30.5 ± 0.5 mV, due to deprotonation of surface hydroxyl groups on the surface silicon (Si) and aluminum (Al) atoms. This is comparable to the findings for other supplementary cementitious materials including microsilica particles (silica fume), which exhibit a zeta potential of −17 mV when dispersed in water [17,53]. As the pH of the solution increases, the zeta potential becomes more negative, which indicates increased stability of the colloidal dispersion. This can be due to the higher concentration of $OH^-$ ions in the solution making these more available to adsorb onto metakaolin surfaces [24,54], and an increase in the deprotonation of surface hydroxyl groups [17]. Therefore, the magnitude of zeta potential becomes increasingly negative as the pH increases up to 12 ($[OH^-] = 10^{-2}$ M), before becoming less negative at higher pH values. The zeta potential reaches its greatest negative magnitude at pH of 12 (−66.3 ± 1.3 mV and −61 ± 1.6 mV for NaOH and KOH, respectively), which implies that the metakaolin dispersions are most stable under these conditions [54]. Beyond pH 12, the zeta potential magnitudes became less negative, indicating the reduction of colloidal stability. However, the isoelectric point (IEP), i.e. the pH value at which the magnitude of positive and negative surface charges are equal, is not reached. This may be because the charge-determining hydroxyl groups remain deprotonated in the highly alkaline medium, meaning that the surface charge of the metakaolin particles remains negative.

It is well known that when the concentration of $OH^-$ ions is high enough, alkali-activation of metakaolin takes place. This involves dissolution of Si and Al from the metakaolin particles, until the concentration of Si and Al in solution is sufficiently high that a polycondensation reaction occurs which leads to the forma-

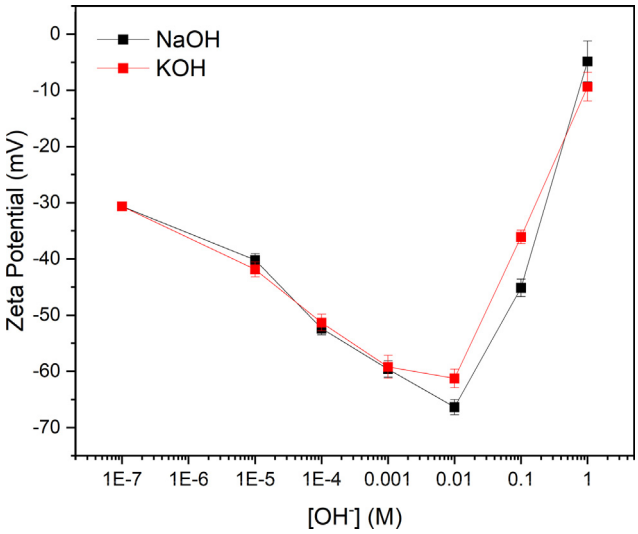


**Fig. 4.** Comparison between the experimentally measured zeta potentials of metakaolin particles in water as a function of hydroxide ion molar concentration, when pH is adjusted by addition of sodium hydroxide (NaOH) and potassium hydroxide (KOH). The error bars show standard error of five repeated measurements (consisting of 30 runs) for each sample.

tion of an alkali aluminosilicate hydrate gel [1,4]. The structure of this gel is a three-dimensional framework formed by $SiO_4$ and $AlO_4^-$ tetrahedra linked by corner-shared oxygen atoms [55–57]. Alkali cations from the activator solution are typically present in octahedrally coordinated sites in this framework to balance the negative charge of the tetrahedrally coordinated aluminum ions [58].

At high pH, the $OH^-$ ions break the interlayer and intralayer bonds in metakaolin, causing its dissolution, thereby providing the constituents necessary to form the aluminosilicate geopolymer network through polycondensation (geopolymerization) reactions [59]. In contrast, at lower pH, the concentration of $OH^-$ is not sufficient to induce a high rate or extent of metakaolin dissolution, and so an extensive alkali-aluminosilicate network does not form. In the work presented here, increasing pH and concentration of $OH^-$ ions in the metakaolin dispersions results in an increase in the rate of dissolution of metakaolin.

In the systems studied here, the zeta potential measurements indicate that dissolution of metakaolin occurs when pH > 12. This decreases the magnitude of the negative zeta potential values, and reduces stability of the colloidal dispersion. Additionally, in alkali-activation, the metal cations ($Na^+$/$K^+$) are incorporated into the alkali-aluminosilicate network structure. Hence, the zeta potential magnitude is reduced. These results indicate that both monovalent cations ($Na^+$ and $K^+$) adsorb onto metakaolin surfaces to a similar degree, with $K^+$ resulting in negative zeta potentials of slightly lower magnitudes at pH 12 and 13. The general trend in zeta potentials of metakaolin particles as a function of pH adjusted by either NaOH or KOH, remained unchanged. This can be due to the adsorption of these cations on metakaolin surfaces mainly being driven by coulombic interactions. This is comparable to the findings for other silicate surfaces, including quartz particles, where KCl resulted in lower negative zeta potentials, compared to NaCl as a function of solution pH (3–11) [60]. This indicated that $K^+$ cations adsorbed in higher quantities than $Na^+$ cations, and were more effective in screening the negative surface charge of the quartz particles. This observation was attributed to the presence of additional nonelectrostatic interaction between the surface and the ions [60].

### 3.1.2. Effect of divalent cations in electrolytes

Zeta potential of metakaolin surfaces were measured as a function of electrolyte ($MgCl_2$ and $CaCl_2$) concentration (0–0.1 M) at constant pH (NaOH and KOH) of 13, to investigate the effect of divalent cations on surface charge modification of metakaolin particles in high alkaline environment. Zeta potential values of metakaolin surfaces as a function of $MgCl_2$ and $CaCl_2$ aqueous electrolyte concentration at pH 13 are shown in Fig. 5. The results presented in section 3.1.1 for zeta potential of the dispersions in the absence of divalent cations indicated that the metakaolin system was most stable at pH at 12 (negative zeta potential of greatest magnitude). However, a pH of 13 was selected in this section, as this is more representative of alkali-activation conditions, while remaining stable.

The zeta potentials of metakaolin particles in the presence of divalent cationic electrolyte solutions ($CaCl_2$, $MgCl_2$) at constant pH adjusted by both NaOH and KOH showed similar behavior, irrespective of the specific ionic species present (Fig. 5). Increasing the concentration of the divalent cations ($Ca^{2+}$ and $Mg^{2+}$) reversed the sign of zeta potential from negative to positive and then increased the positive magnitude of zeta potential up to a maximum value, before gradually decreasing its magnitude toward zero at the higher electrolyte concentrations tested.

As can be seen in Fig. 4, the metakaolin particles have negative surface charges in the absence of divalent cations, due to deprotonation of surface hydroxyl groups and the attachment of $OH^-$ anions onto the metakaolin surface, in the highly alkaline environment. This facilitates adsorption of positively charged cations ($Mg^{2+}$ and $Ca^{2+}$) upon increasing the electrolyte concentration, and the zeta potential magnitude becomes less negative. This decrease in magnitude of zeta potential indicates a contraction of the EDL surrounding the metakaolin particles, and that the colloidal systems are becoming less stable. The point of zero charge (PZC), i.e. the concentration of potential determining ions at which the surface charge of the particle is equal to zero, is achieved at electrolyte concentrations between 1 and 10 mM. The change in sign of the zeta potential demonstrates the charge-determining nature of these cations and suggests that the $Ca^{2+}$ and $Mg^{2+}$ cations are specifically adsorbing onto the inner (Stern) layer of the EDL [61], increasing the repulsive electrostatic forces. This specific adsorption is suggested to be due to ionic interactions mainly driven by coulombic forces [15]. The adsorption of cations reaches an equilibrium at monolayer concentration of 30 mM and 20 mM in NaOH and KOH systems, respectively, where the maximum positive surface charge is reached.

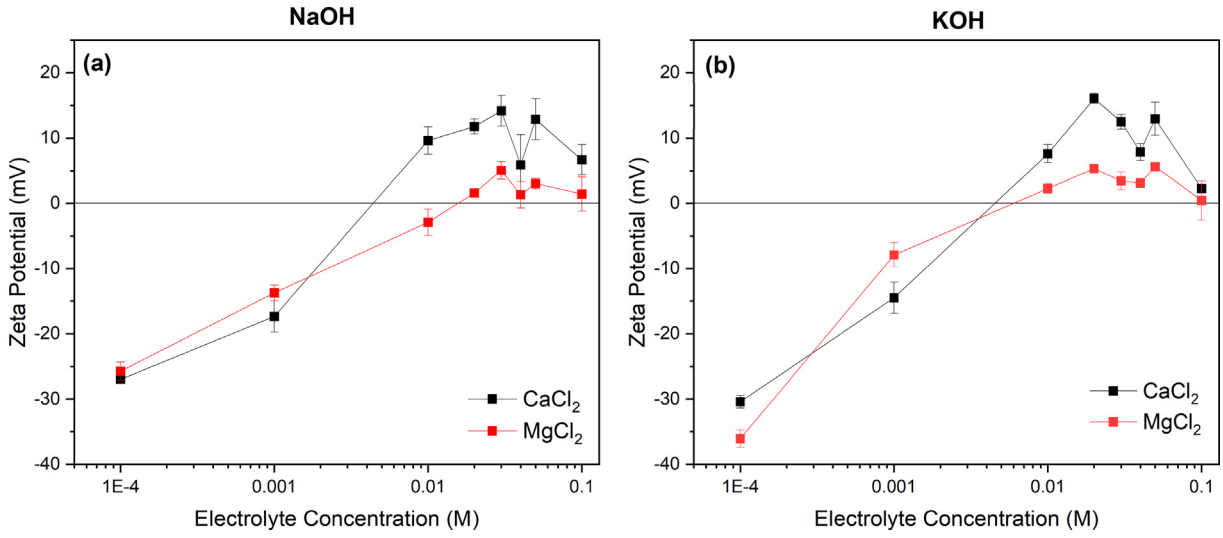


**Fig. 5.** Comparison between the experimentally measured zeta potential values for metakaolin particles in water as a function of aqueous electrolyte (calcium chloride ($CaCl_2$) and magnesium chloride ($MgCl_2$)) molar concentrations, at a constant pH of 13, adjusted by sodium hydroxide (NaOH) (a) and potassium hydroxide (KOH) (b). The error bars show standard error of five repeated measurements (consisting of 30 runs) for each sample.

It has previously been shown [17] that the adsorption of divalent cations (e.g. $Ca^{2+}$) on spherical mineral surfaces, e.g. microsilica particles, reached a maximum value and then stabilized. This is indicative of an adsorption plateau for the saturated amount of $Ca^{2+}$ ions, which reflects a Langmuir type isotherm. This is typical for monolayer adsorption where there is no interaction between adsorbed species, and the adsorbed species are immobile and are in equilibrium with desorbed species [62]. However, in this study, the zeta potential measurements of metakaolin particles with increasing concentrations of divalent cations ($Mg^{2+}$ and $Ca^{2+}$) showed a presence of secondary peaks at 50 mM $(Ca,Mg)Cl_2$ electrolyte concentration. This may be due to the non-spherical, plate-like shape of metakaolin particles, which may result in differing zeta potential values and/or adsorption tendencies when measured on the particle surface and on the particle edge, resulting in two apparent maxima in the positive magnitudes of zeta potential. Similarly, in a previous study zeta potential of metakaolin particles as a function of solution pH were measured, and the authors reported observation of two IEP values [24]. This was attributed to the charge distribution heterogeneity on the platelet surfaces, where faces and edges may present different charges depending on the suspension pH. Alternatively, the secondary peak may be due to increased precipitation by increasing electrolyte concentrations, approaching saturation with respect to alkali earth hydroxide phases.

Further increase in electrolyte concentration beyond the monolayer concentration resulted in screening of surface charges, and hence a continuous reduction in magnitude of zeta potential was observed. This illustrates the contraction of the EDL as the system became less stable and attractive van der Waals forces became dominant, reflecting the predictions of the DLVO (Derjaguin, Landau, Verwey and Overbeek) theory [63]. This can be due to accumulation of divalent cations around the negatively charged metakaolin particles screening or weakening the net surface charge of the particle [63,64]. By increasing salt concentration, the Debye length is reduced, and the electrostatic repulsion is subsequently screened. Hence, the energy barrier required to attain the primary minimum potential energy is reduced, and the tendency of the system to coagulate increases [65].

When comparing different ionic species, in both NaOH and KOH systems, $CaCl_2$ resulted in positive zeta potential values of greater magnitude compared to $MgCl_2$. This could suggest that $Ca^{2+}$ cations are more effective than $Mg^{2+}$ at adsorbing onto the metakaolin surfaces. It also reinforces the relative insignificance of which alkali hydroxide solution is used to set pH, as the electrostatic interactions of the two monovalent cations tested are similar. Greater specific adsorption of $Ca^{2+}$ ions than $Mg^{2+}$ ions can be due to the smaller hydrated radius of $Ca^{2+}$ [63], which affects its interaction with the metakaolin surfaces. Calcium and magnesium ions contain the same number of ionic charges, while magnesium has a smaller ionic radius, thus its charge is distributed over a smaller volume, generating a higher charge density. This leads to exertion of stronger attractive forces on the dipoles of water molecules and formation of a larger hydrated shell for $Mg^{2+}$ ions. Therefore, a smaller hydrated ionic radius of $Ca^{2+}$ enables the cations to approach the surface of the metakaolin particles more readily and become specifically adsorbed. Similar behavior was observed by Saka & Guler [61] when $Ca^{2+}$ and $Mg^{2+}$ cations interacted with clay surfaces.

### 3.1.3. Effect of superplasticizer dosage

Zeta potentials of metakaolin surfaces as a function of superplasticizer dosage at constant electrolyte ($CaCl_2$ and $MgCl_2$) concentration and pH (NaOH and KOH) were measured to ascertain optimum concentration and conditions for superplasticizer operation to achieved dispersion in these systems. Fig. 6 shows zeta potential values of metakaolin particles as a function of SNSFP dosage (0–5 wt.% relative to the mass of metakaolin powder) at constant $MgCl_2$ and $CaCl_2$ aqueous electrolyte concentrations and constant solution pH (13). In NaOH systems without superplasticizers (Fig. 5), the highest positive magnitude of zeta potential was observed at an electrolyte concentration ($CaCl_2$ or $MgCl_2$) of 30 mM, while in KOH systems, this value was observed at 20 mM of $CaCl_2$ or $MgCl_2$ in KOH systems. Therefore, the electrolyte concentrations were kept constant at 30 mM in NaOH solutions and 20 mM in KOH solutions in the experiments depicted in Fig. 6, providing the optimum potential for interaction and electrostatic adsorption of anionic superplasticizer molecules onto the positively charged metakaolin surfaces.

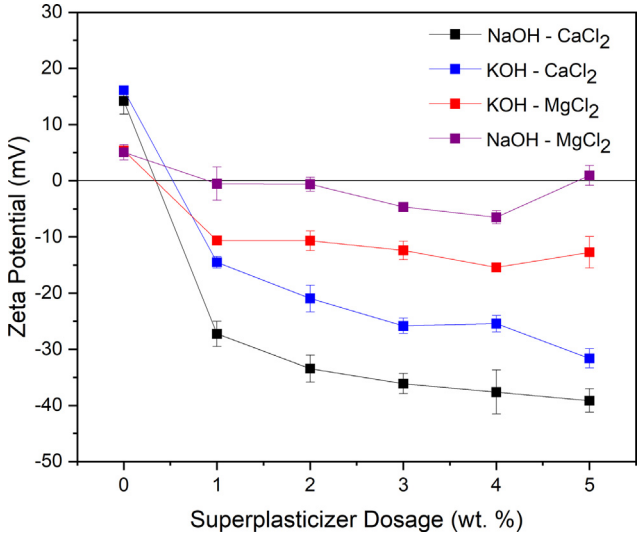


**Fig. 6.** Experimentally measured zeta potentials of metakaolin particles in water as a function of SNSFP superplasticizer dosage (1–5 wt.%), at constant pH 13, adjusted by sodium hydroxide (NaOH) and potassium hydroxide (KOH) and at constant calcium chloride ($CaCl_2$) and magnesium chloride ($MgCl_2$) aqueous electrolyte concentrations (30 mM in NaOH and 20 mM in KOH). The error bars show standard error of five repeated measurements (consisting of 30 runs) for each sample.

Naphthalene sulfonate-based superplasticizers are designed to interact with cementitious particles to cause their dispersion via electrostatic repulsion. In this superplasticizer, the polar, hydrophilically functionalized hydrocarbon chain of the polymer adsorbs onto the cement particle and imparts a strong negative charge, making the cement particle hydrophilic. This leads to reduction of surface tension of the surrounding water and enhances fluidity [7].

The data show that the zeta potential of metakaolin surfaces, which is positive in the absence of the SNSFP and the presence of divalent cations ($Mg^{2+}$ or $Ca^{2+}$), reverses to negative values by addition of the superplasticizer to the suspension. This is due to interaction of this anionic admixture and its adsorption onto the diffuse layer of the EDL surrounding the metakaolin particle through the cations ($Mg^{2+}$ or $Ca^{2+}$) previously adsorbed in the Stern layer. The increasing magnitude of zeta potential by increasing dosage of SNSFP superplasticizer reflects the expansion of the EDL and increased electrostatic repulsion between the particles. Once this adsorption reaches equilibrium, a further increase in dosage of superplasticizer either reduces the negative magnitude of zeta potential or results in an adsorption plateau.

The change in sign of zeta potential upon addition of SNSFP demonstrates the charge-determining nature of the superplasticizers, as the metakaolin surface charge is reversed even at the lowest dosage. This is particularly evident in the NaOH-$CaCl_2$ sys-

tem where addition of only 1 wt.% SNSFP superplasticizer resulted in strong negative surface charges (−27.2 ± 2.2 mV). This negative magnitude was further amplified by increasing the superplasticizer dosage to 5 wt.%, yielding zeta potentials as negative as −39.1 ± 2.1 mV. Superplasticizers are intended to increase the dispersion of the cement particles and break down flocs, resulting in release of the entrapped water, thereby improving workability [8].

Similar trends were observed in the presence of other ionic species whilst achieving different degrees of adsorption and dispersion effects. The metakaolin in aqueous solutions containing $CaCl_2$ attained a greater degree of stability, compared to the solutions containing $MgCl_2$, as demonstrated by higher negative magnitudes of the zeta potential values observed across the dosage range. This can be due to initially higher positive zeta potential measured in the presence of $CaCl_2$ before addition of SNSFP. This provided a greater electrostatic attraction between SNSFP molecules and the metakaolin surface, and subsequently a greater degree of adsorption. For both NaOH-$CaCl_2$ and KOH-$CaCl_2$ systems, increasing dosage of SNSFP superplasticizer up to 5 wt.% did not show that a maximum in stability was reached in this concentration range (i.e. the zeta potential decreased monotonically), whereas a maximum in dispersion (local minimum in zeta potential) for both NaOH-$MgCl_2$ and NaOH-$MgCl_2$ systems was observed at dosage of 4 wt.%. Comparing the effect of NaOH against that of KOH in the presence of $CaCl_2$ or $MgCl_2$, in $CaCl_2$ systems, the negative zeta potential values are of greater magnitude (i.e. more negative) when in the presence of NaOH (black line, Fig. 6) compared with KOH (blue line, Fig. 6), while in $MgCl_2$ systems, negative zeta potential values are of greater magnitude (i.e. more negative) in the presence of KOH (red line, Fig. 6). When comparing the effect of $CaCl_2$ against that of $MgCl_2$ in the presence of NaOH or KOH, in the presence of SNSFP the negative zeta potential values are of greater magnitude (i.e. more negative) in the presence of $CaCl_2$ than in the presence of $MgCl_2$. This indicates that $CaCl_2$ was more efficient in increasing dispersion in the presence of NaOH, while $MgCl_2$ resulted in the greatest stability in KOH systems. These results highlight the differing surface interactions that occur in these alkali-activated systems and the presence of different type of mono- and divalent cations at the mineral-water interfaces, affecting the adsorption of polymers, and hence the colloidal stability and dispersion effect.

The influence of different alkali metal cations on adsorption of a polymer onto quartz surfaces was previously investigated using zeta potential measurements [60], where the presence of less-hydrated cations, also known as water structure breakers ($Cs^+$ and $K^+$) significantly enhanced the adsorption density of the polymer, compared to strongly hydrated cations, also known as structure makers ($Li^+$ and $Na^+$). Additionally, the adsorption of ions at oxide-solution interfaces was investigated using a thermodynamic model [66], where it was discussed that the low dielectric oxide surfaces will preferably interact with less hydrated cations, whereas strongly hydrated ions were predicted to be able to more easily adsorb on oxide surfaces with high dielectric constant. These variations were attributed to the ability of the metal ion to exchange its secondary hydration shell for the interfacial water when approaching the surface, assuming that adsorption takes place in the inner Helmholtz plane of the double layer. In the current study, it was observed that the less hydrated alkaline earth cation ($Ca^{2+}$) resulted in negative zeta potential values of significantly higher magnitude on the surface of metakaolin in the presence of the SNSFP superplasticizer, when compared to the more hydrated $Mg^{2+}$ cation. This indicates the ability of the less hydrated $Ca^{2+}$ to approach the aluminosilicate surface layer of metakaolin more readily, and facilitate adsorption of the polymer on its surface.

### 3.1.4. Effect of pH on stability of dispersions

To examine the stability of the colloidal dispersion over a range of pH, the zeta potential of metakaolin particles was measured as a function of $OH^-$ concentration from $10^{-3}$ M (pH 11) to 1 M (pH 14), adjusted by NaOH, at a constant dosage of SNSFP superplasticizer (5 wt.% relative to the mass of metakaolin powder) and constant $CaCl_2$ aqueous electrolyte concentration (30 mM); the results of this experiment are shown in Fig. 7. These conditions reflect those of the most stable system (highest negative magnitude of zeta potential) across the range of superplasticizer dosage examined in Fig. 6. Insolubility of superplasticizers, followed by chemical instability in the highly alkaline environment (pH > 12) due to changes in their molecular structure, have previously been suggested to be the two major challenges hindering their operation in alkali-activated cements [42,43]. This experiment therefore examines the stability of the metakaolin dispersion in the presence of SNSFP by varying pH.

The results in Fig. 7 show that by increasing solution pH, the zeta potential of metakaolin surfaces becomes increasingly negative, due to expansion of the EDL surrounding the particles and increased electrostatic repulsion. The highest negative magnitude of zeta potential was observed at a pH of 13 (−32.5 ± 1.8 mV), indicating the stability of the colloidal system. This is a desirable outcome as it signifies that the SNSFP remains stable in a highly alkaline environment. There is a slight reduction in the magnitude of zeta potential between pH values of 13 and 14 (−24.8 ± 1.7 mV), suggesting the contraction of the EDL surrounding the metakaolin particles, and hence, reduced stability of the colloidal dispersion. However, this does not overcome the ability of SNSFP superplasticizer to provide a dispersion effect at high pH, as the reduction in magnitude of zeta potential is relatively small. Furthermore, the results indicated that SNSFP is soluble in the highly alkaline environment, as reflected by increased electrostatic repulsion, which is the mechanism of operation for the second generation of superplasticizers. However, the slight reduction in zeta potential at a pH of 14 could indicate partial insolubility (or other causes of partial loss of function) of SNSFP in the most highly alkaline environments tested.

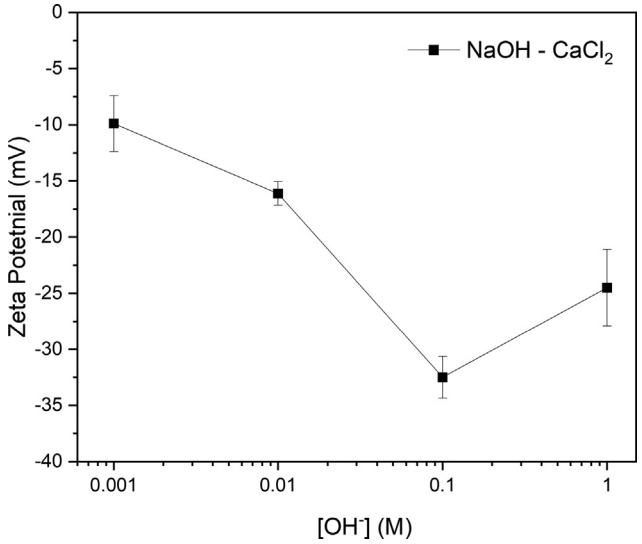


**Fig. 7.** Experimentally measured zeta potentials of metakaolin particles in water as a function of hydroxide ions molar concentration, adjusted by sodium hydroxide (NaOH), at constant dosage of SNSFP superplasticizer (5 wt.%) and calcium chloride ($CaCl_2$) aqueous electrolyte concentration (30 mM). The error bars show standard error of five repeated measurements (consisting of 30 runs) for each sample.

The current results indicate that the metakaolin particles were most stable at pH of 13 in the presence of SNSFP, which differs from the most stable pH (12) of metakaolin surfaces in the absence of SNSFP and divalent cations ($Mg^{2+}$ or $Ca^{2+}$). This suggests that SNSFP is particularly effective in an alkaline environment given the presence of specific concentrations of divalent cations, while contributing toward increased stability of the colloidal system.

### 3.2. Total organic carbon content

TOC content measurements were employed to evaluate the amount of non-adsorbed naphthalene sulfonate-based superplasticizer remaining in the solution after each adsorption experiment, using the depletion method by assuming that the interaction is due merely to surface adsorption. The percentage of adsorbed amount of SNSFP on metakaolin surfaces relative to the control samples was calculated from the difference between the TOC content of the positive control solutions (100%) and the colloidal dispersions for each sample (the non-adsorbed amount (%)).

The adsorbed amount of SNSFP at constant dosage of 5 wt.% relative to the mass of metakaolin powder at constant pH 13 under different aqueous solution environments, including NaOH-$CaCl_2$, NaOH-$MgCl_2$, KOH-$CaCl_2$, KOH-$MgCl_2$, was measured in order to evaluate the effect of different ionic species on the degree of adsorption of the superplasticizer onto mineral surfaces, as shown in Fig. 8a. At high superplasticizer concentrations (0.05 g/l), SNSFP adsorbed onto the metakaolin particles most effectively in the NaOH-$CaCl_2$ system (68.8%), followed by KOH-$CaCl_2$ (64.25%), while adsorption of SNSFP onto the metakaolin particles in KOH-$MgCl_2$ and NaOH-$MgCl_2$ systems were less effective (35% and 25%, respectively). This observation is consistent with our zeta potential results where the positive magnitude of the zeta potential in the system was altered to the largest negative magnitude in NaOH-$CaCl_2$ ($-39.1 \pm 2.1$ mV), followed by KOH-$CaCl_2$ ($-31.6 \pm 1.7$ mV), when SNSFP was added at dosage of 5 wt.% (Fig. 6), while zeta potential values in KOH-$MgCl_2$ and NaOH-$MgCl_2$ systems were only $-12.7 \pm 2.7$ mV and $0.9 \pm 1.7$ mV, respectively. This confirms that the superplasticizer adsorbed in higher quantities in NaOH-$CaCl_2$ and KOH-$CaCl_2$ systems and was more effective in providing a dispersion effect and screening the positive surface charge of the metakaolin particles. Thus, a comparison between zeta potential and TOC results across the range of examined ionic species, clearly illustrates the influence of different mono and divalent cations present in the aqueous solution on the degree of adsorption of SNSFP onto mineral surfaces, showing a similar adsorption trend using both techniques.

The mass of total organic carbon remaining in the SNSFP solution (relative to the control samples) after adsorption onto metakaolin surfaces at constant pH (NaOH) of 13 and $CaCl_2$ concentration of 30 mM, as a function of superplasticizer dosage (1–5 wt.% relative to the mass of metakaolin powder), are shown in Fig. 8b. These conditions (NaOH-$CaCl_2$) reflect those of the most stable system across the range of examined ionic species (Fig. 6). As can be seen from Fig. 8b, the TOC content measurement indicates that the mass of total organic carbon remaining in the SNSFP solution increases slightly with increasing the superplasticizer dosage from 1 to 2 wt.% with non-adsorbed amount of 0.72 % and 4.1 %, respectively. However, the mass of total organic carbon remaining in the SNSFP solution reaches a plateau beyond the dosage of 3 wt.% with non-adsorbed amount of 32% whilst remaining almost unchanged at dosages of 4 and 5 wt.% (non-adsorbed amount of 34.36 % and 33.53 %, respectively). This observation is consistent with our zeta potential measurement results as a function of SNSFP dosage (Fig. 6), where the negative magnitude of zeta potential in system rapidly increased by increasing the superplasticizer dosage from 0 to 3 wt.% by approximately 50 mV, while a further increase in dosage of the SNSFP between 3 wt.% and 5 wt.% resulted in a gradual increase in magnitude of zeta potential only by 10 mV. This observation confirms that the SNSFP reached an adsorption plateau in in NaOH-$CaCl_2$ system beyond dosage of 3 wt.% using both zeta potential and TOC analysis. The current TOC results provide further insight into the presence of specific ionic species and the optimum dosage of superplasticizer required to provide an effective dispersing effect before achieving an adsorption equilibrium under a wide range of conditions representing alkali-activated systems.

### 3.3. Fourier transform infrared spectroscopy

ATR-FTIR spectra of solid phase pure unreacted metakaolin and SNSFP superplasticizer samples were measured. Additionally, solid phase FTIR spectroscopy of metakaolin plus any adsorbed SNSFP

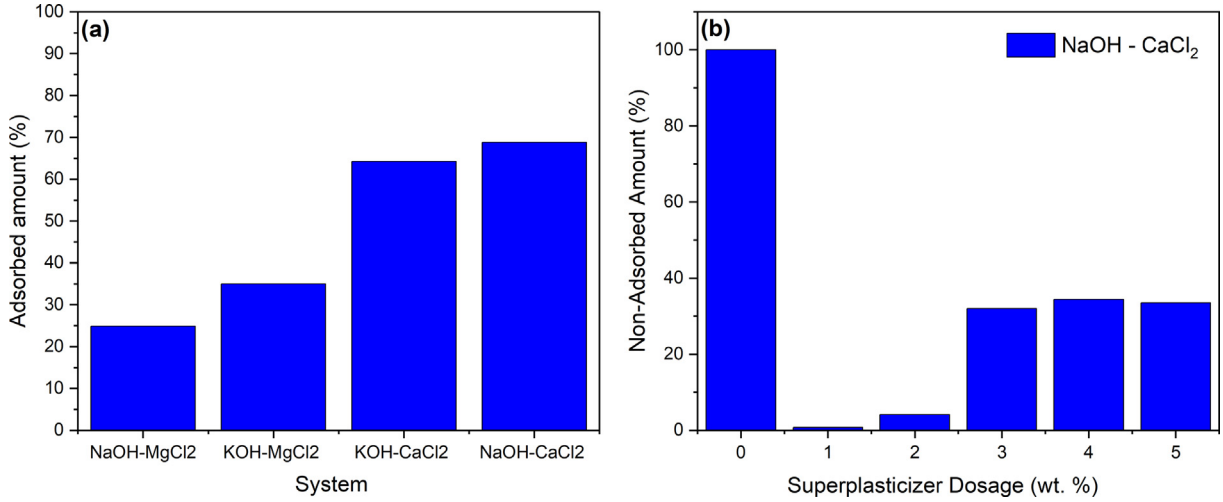


**Fig. 8.** (a) The calculated adsorbed amount of SNSFP (relative to the respective control samples) at constant superplasticizer dosage of 5 wt.% in different aqueous solutions at constant pH 13, adjusted by sodium hydroxide (NaOH) and potassium hydroxide (KOH) and at constant calcium chloride ($CaCl_2$) and magnesium chloride ($MgCl_2$) aqueous electrolyte concentrations (30 mM in NaOH and 20 mM in KOH). (b) Experimentally measured mass of total organic carbon remaining in SNSFP solution (relative to the respective control samples) at constant pH (13), adjusted by sodium hydroxide (NaOH) and calcium chloride ($CaCl_2$) aqueous electrolyte concentration (30 mM) as a function of superplasticizer dosage (1–5 wt.%). The zero-superplasticizer bar shows the normalized TOC measurement of the positive control solution (100%).

remaining after filtration of the metakaolin suspensions (*ex situ*), and liquid phase FTIR spectroscopy of the metakaolin suspensions *in situ* at constant superplasticizer dosage of 5 wt.%, constant pH 13, adjusted by NaOH and KOH, and constant $CaCl_2$ and $MgCl_2$ aqueous electrolyte concentrations (30 mM in NaOH and 20 mM in KOH) were measured. ATR-FTIR data can be used to confirm the presence of SNSFP adsorbed on the surface of metakaolin in the presence of examined ionic species. Fig. 9 presents FTIR spectra of the pure unreacted metakaolin and SNSFP powders used in this study. The ATR-FTIR spectrum for unreacted metakaolin exhibits a high intensity band at 1068 $cm^{-1}$ which is attributed to asymmetric stretching of Si–O–T bonds, where T is either aluminum (Al) or silicon (Si) in tetrahedral coordination [67]. Additionally, the low intensity band at 797 $cm^{-1}$ is assigned to symmetric stretching of Si–O–T bonds [67]. The ATR-FTIR spectrum of unreacted SNSFP consists of the aromatic ring modes at 1641, 1597 and 1507 $cm^{-1}$, the sulfonate group bands at 1180 and 1040 $cm^{-1}$, and the methylene C–H bending vibration at 1450 $cm^{-1}$ [68].

As can be seen from Fig. 10a, no additional adsorption peaks related to the SNSFP in the filtered powder FTIR spectra were observed, as the adsorption bands associated with sulfonate group were covered by the high intensity asymmetric stretching of Si–O–T bonds of metakaolin. This demonstrates the need for analysis of the dispersions *in situ* (liquid phase), as shown in Fig. 10b. The high intensity bands located at 1635 $cm^{-1}$ is associated with water O–H–O scissors bending vibration, and the low intensity band at 2120 $cm^{-1}$ is the result of coupling of the bending vibrations and a broad liberation band in the near-infrared [69]. The addition of SNSFP superplasticizer to the metakaolin colloidal dispersion results in the observation of sulfonate group adsorption bands. A broad adsorption band located in range of 1010 to 1260 $cm^{-1}$ is associated with the sulfonate group [68] and confirms the presence of SNSFP adsorbed on the surface of metakaolin. This adsorption bands are more apparent in NaOH-$CaCl_2$ and KOH-$CaCl_2$ systems, which have shown to be the most disperse systems in the range of examined ionic species using zeta potential. The observation of sulfonate group bands in the Ca-modified systems provides direct evidence for Ca-mediated adsorption of SNSFP, while this is not apparent to the same extent in Mg-mediated systems. This likely results from the lower charge density of $Ca^{2+}$ cations than $Mg^{2+}$, allowing the $Ca^{2+}$ cations to approach the surface of the metakaolin particles more readily, and facilitating the adsorption of SNSFP onto the metakaolin surfaces. Additionally, TOC measurements also confirmed lower organic contents remaining in the NaOH-$CaCl_2$ and KOH-$CaCl_2$ solutions, confirming higher adsorptions of the superplasticizer onto metakaolin surfaces in the presence of these ionic species.

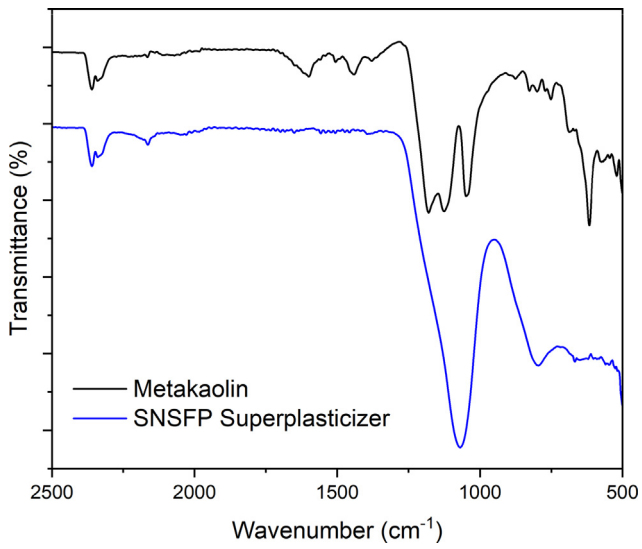


**Fig. 9.** Solid phase ATR-FTIR spectra of the pure unreacted metakaolin and SNSFP superplasticizer samples used in this study.

### 3.4. Proposed mechanisms

Based on the findings presented here, there are several mechanisms elaborated to describe flowability of metakaolin-based alkali-activated systems. Flowability of cementitious systems is highly dependent on colloidal interactions at solid-liquid interfaces as they drive the adsorption capacity of surface-active admixtures, e.g. superplasticizers, on cementitious surfaces during the early stage of hydration. The DLVO theory describes the stability of colloidal particles in a suspension, based on long-range interaction forces (van der Waals and electrostatic) and the bulk properties of a solvent, whereas it neglects the natural properties of a molecule, such as shape, chemistry and size [70].

CC contain a considerable area of silicate- and aluminate-terminated surfaces, which are negatively charged in a highly alkaline environment. The specific adsorption of divalent cations ($Ca^{2+}$ and $Mg^{2+}$) in the Stern layer of the EDL surrounding negatively charged metakaolin particles facilitates electrostatic adsorption of anionic sulfonates in the superplasticizers within the diffuse layer, generating a negative charge on the particles [71–74]. This mechanism is also known as multicomponent ionic exchange (MIE) and is attributed to the exchange of ions, including adsorption of potential-determining cations and co-adsorption of anionic species, resulting in reduction of the ionic bonding between superplasticizer molecules and particle surfaces. According to the mechanism of MIE, divalent cations ($Ca^{2+}$ and $Mg^{2+}$) adsorb onto the negatively charged surfaces, increasing the positive surface charge density [75]. This minimizes electrostatic repulsive forces, and results in co-adsorption of anionic superplasticizer polymers. Similar behavior was observed when studying the interactions between polycarboxylate-based superplasticizers and GGBFS in synthetic cement pore solution [20]. It was suggested that the adsorption of $Ca^{2+}$ ions on the initially negatively charged slag surfaces in highly alkaline media, and subsequent adsorption of sulfate ions present in synthetic cement pore solution, provides a competitive adsorption between the superplasticizers and $SO_4^{2-}$ ions, creating a strong dispersion effect. The anionic charge density of the polymer, specific surface area and surface charge of each mineral type and the packing density of $Ca^{2+}$ ions adsorbed on the surfaces, were identified as the driving factors in the adsorption of polymer onto the cementitious surfaces and the resultant efficacy of dispersion [17,21].

Additionally, when polymers are interacting with $Ca^{2+}$ and $Mg^{2+}$ ions, the process involves the removal of the hydration water and replacement of the ion at the binding site of the metakaolin surfaces [76]. It should be noted that these ions are constituent of a dynamic system in which the relative concentrations of all the species are continually changing, which results in competitive adsorption of ions present in the cement pore solution. The SNSFP molecules compete with water for metakaolin surface sites. Less-hydrated cations disturb the interfacial water structure around metakaolin particles. Hence, allowing the SNSFP to approach the amorphous gel-like surface layer of metakaolin more readily and interact with the surface groups. In the current study, it was observed that presence of different mono- and divalent cations resulted in different magnitudes of zeta potential, and thereby different degrees of polymer adsorption. This is attributed to variation in surface charge density and hydrated radius of these cations and their ability to penetrate surface layer of metakaolin particle, thereby controlling competitive adsorption of the SNSFP on these

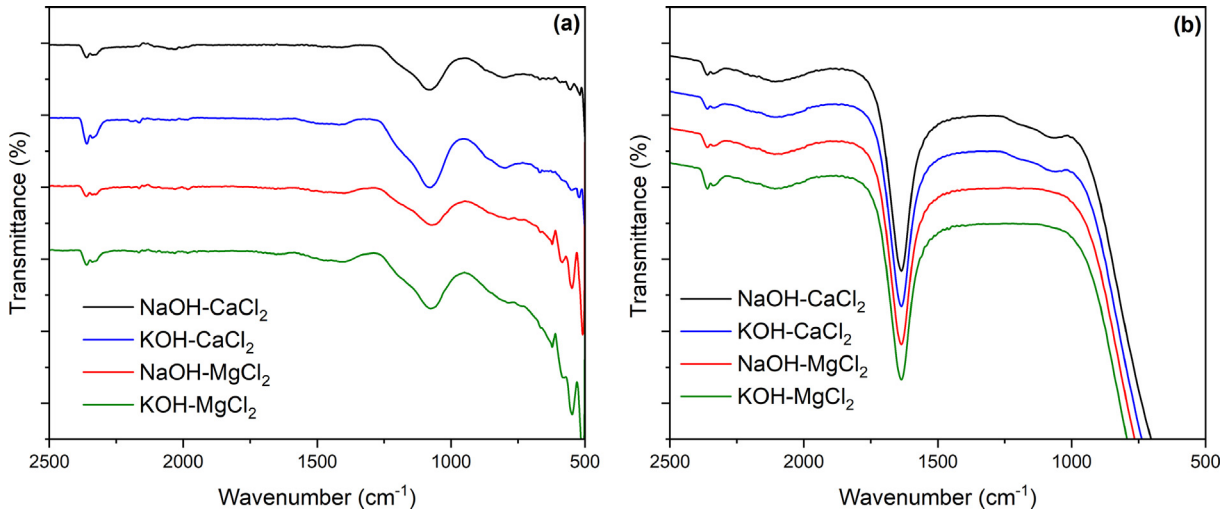


**Fig. 10.** (a) Solid phase FTIR spectra of metakaolin plus any adsorbed SNSFP remaining after filtration of the metakaolin suspensions ex situ at constant superplasticizer dosage of 5 wt.%, constant pH 13, adjusted by sodium hydroxide (NaOH) and potassium hydroxide (KOH), and constant calcium chloride ($CaCl_2$) and magnesium chloride ($MgCl_2$) aqueous electrolyte concentrations (30 mM in NaOH and 20 mM in KOH). (b) Liquid phase ATR-FTIR spectra of the metakaolin suspensions *in situ* at constant superplasticizer dosage of 5 wt.%, constant pH 13, adjusted by sodium hydroxide (NaOH) and potassium hydroxide (KOH), and constant calcium chloride ($CaCl_2$) and magnesium chloride ($MgCl_2$) aqueous electrolyte concentrations (30 mM in NaOH and 20 mM in KOH).

surfaces. Similarly, the adsorption of various alkali and alkaline earth metal cations on silicate surfaces, e.g. quartz, was investigated by Allen et al. [77] using flow adsorption microcalorimetry and *in situ* pH measurements. It was found that the magnitudes of the heats of adsorption and exchange reactions increased along the Hofmeister series ($Li^+ < Na^+ < K^+ < Rb^+ < Cs^+$ and $Mg^{2+} < Ca^{2+} < Sr^{2+} < Ba^{2+}$), which showed strong correlation to hydration properties, e.g. bulk cation hydration enthalpy and hydrated radius. The authors concluded that for both alkali and alkaline earth cations, interactions with the quartz surface through either adsorption or exchange reactions implicate processes involving their hydration shell.

Therefore, as a result of blocking of reactive sites, the electrostatic double layer and hydrated water molecules formed promote repulsive forces between the metakaolin particles. The attractive van der Waals forces between the metakaolin surfaces are disturbed, which result in the disjoining pressure becoming more positive, leading to more stable colloidal systems and preventing particles from adhering to one another to form aggregates [78–80]. Therefore, all of these interfacial forces, including both DLVO and non-DLVO forces have a contribution in stability of the colloidal system by contributing toward the disjoining pressure.

In addition to the adsorbed amount of superplasticizer which determines the dispersion effect and initial fluidity, the presence of non-adsorbed co-dispersants polymers is also vital in controlling time-dependent fluidity properties (slump retention) by facilitating the dispersion of newly formed hydrated phases [14]. The non-ionic molecules which do not adsorb onto cementitious particles but remain dissolved in the pore solution, act as co-dispersants by inducing repulsive depletion forces which prevent cement particles from agglomeration [14].

## 4. Conclusions

The surface interactions of a commercial superplasticizer (sodium naphthalene sulfonate formaldehyde polymer (SNSFP)) with metakaolin particles in model alkali-activated systems under a varied range of conditions, including pH (7–14), ionic composition ($Na^+$, $K^+$, $Ca^{2+}$, and $Mg^{2+}$) and ionic concentration (0–100 mM), were systematically examined by adsorption measurements using experimental zeta potential and total organic carbon content analysis. The following can be concluded:

- The metakaolin particles are strongly negatively charged in water (−30 mV).
- Metakaolin surfaces in KOH and NaOH solutions are most stable at a pH of 12, evidenced by the negative zeta potential of greatest magnitude (−66 mV and −61 mV, respectively), and remained stable at pH of 13 (−45 mV and −36 mV, respectively).
- The surface electrostatic charge of metakaolin particles at pH 13 can be reversed from negative to positive by specific adsorption of potential-determining divalent cations, facilitating the adsorption of negatively charged acidic groups of SNSFP superplasticizers via a mechanism of multicomponent ionic exchange (MIE).
- $Ca^{2+}$ ions resulted in positive zeta potential of greater magnitudes compared to $Mg^{2+}$ (14 mV and 5 mV, respectively). Therefore, SNSFP superplasticizers are more effective at dispersing the metakaolin particles in the presence of $CaCl_2$ compared to $MgCl_2$, irrespective of the type of monovalent ions ($Na^+$ or $K^+$) present.
- The optimal conditions for effective adsorption of SNSFP superplasticizer on metakaolin surfaces in a highly alkaline environment (pH 13), are 30 mM $CaCl_2$, with NaOH, at a SNSFP dosage of 5 wt.%.
- Total organic carbon measurements confirmed that the SNSFP was most effective in adsorbing onto the metakaolin surfaces in the NaOH-$CaCl_2$ system, followed by the KOH-$CaCl_2$ system.
- Total organic carbon measurements indicated that the adsorption of SNSFP superplasticizer on metakaolin surfaces reaches equilibrium beyond a dosage of 3 wt.% at pH 13 in an NaOH-$CaCl_2$ system.
- Liquid phase Fourier transform infrared spectroscopy of the dispersions *in situ* confirmed the presence of sulfonate group adsorption bands on metakaolin surfaces in NaOH-$CaCl_2$ and KOH-$CaCl_2$ systems.
- The observation of sulfonate group bands in the Ca-modified systems provides direct evidence for Ca-mediated adsorption of SNSFP, while this is not apparent to the same extent in Mg-mediated systems. This results from the lower charge den-

sity of $Ca^{2+}$ cations than $Mg^{2+}$, allowing the $Ca^{2+}$ cations to approach the surface of the metakaolin particles more readily, and facilitating the adsorption of SNSFP onto the metakaolin surfaces.

- The suggested mechanism in this study for colloidal stability and dispersion of metakaolin particles in metakaolin-based alkali-activated systems, in the presence of different ions and highly alkaline media, is changes in the distribution and structure of the electric double-layer, as well as structural forces due to alteration in surface charge density and hydrated shell, facilitating competitive adsorption of the polymer.

This work shows that the presence of different types of mono and divalent ions in the fresh cement reaction mixture can influence the surface interactions and adsorption of superplasticizers on solid precursors in highly alkaline environments. The developed methodology can be employed to approximate the adsorbed and non-adsorbed amount of superplasticizer on surfaces of cementitious particles by direct and indirect measurements, systematically examining dispersion and fluidity of alkali activated systems under a wide range of conditions.

In particular, the direct observation of cation-mediated adsorption of SNSFP onto metakaolin surfaces in the presence of $Ca^{2+}$, but not $Mg^{2+}$, which results from the lower charge density of $Ca^{2+}$ cations compared with $Mg^{2+}$ cations, and the suggested mechanisms , facilitating competitive adsorption of the polymer and providing colloidal stability and dispersion of metakaolin particles in the presence of different ions and highly alkaline media, provides significant new insight, and advances the knowledge established by previously published work in this area [8,10,17,22,23].

This provides important insight into the fundamental processes governing reversible adsorption phenomena in Portland cement-based and alkali-activated cements containing metakaolin, which can exhibit significantly higher fresh state pH than those based solely on Portland cement.

For further fundamental investigations, the effect of charge screening due to increased total electrolyte concentration can also be explored, by eliminating the effect of changes in ionic strength by measuring zeta potential of metakaolin particles as a function of sodium chloride (NaCl) and potassium chloride (KCl), such that the total ionic strength remains constant.

Furthermore, the current experimental design can also be expanded to analyze the interactions between the variables investigated in the current work (e.g. alkaline earth metal ion concentration and pH) by examining the effect of calcium hydroxide ($Ca(OH)_2$), magnesium hydroxide ($Mg(OH)_2$), calcium chloride ($CaCl_2$), and magnesium chloride ($MgCl_2$) on the zeta potential of metakaolin surfaces, providing insight into the influence of specific ionic mixtures on particle zeta potential.

Lastly, surface wettability and surface energy measurements can also be employed to provide an insight in degree of wetting of superplasticizers on cementitious surfaces, and hence the dispersion effect of alkali activated systems. Moreover, atomic force microscopy can be used to directly measure adhesion forces including both DLVO and non-DLVO interactions in aqueous electrolyte solutions and high alkaline media. These surface characterization methods could provide more in-depth fundamental understanding of interfacial forces and dispersing mechanisms involved in this complex organic-modified inorganic system.

**Funding**

This work is co-funded by UKRI Innovate UK, EPSRC and Lubrizol Ltd., through a Knowledge Transfer Partnership (KTP, Ref: 12041) in which The University of Sheffield is a Knowledge Base partner. KTPs aim to help businesses improve their competitiveness and productivity through the better use of knowledge, technology and skills within the UK Knowledge Base partners.

*CRediT authorship contribution statement*

**Maryam H. Derkani:** Conceptualization, Methodology, Validation, Investigation, Visualization, Formal analysis, Writing - original draft, Writing - review & editing. **Nathan J. Bartlett:** Conceptualization, Methodology, Resources, Writing – review & editing, Supervision, Project administration, Funding acquisition. **Gaone Koma:** Investigation, Writing – review & editing. **Laura A. Carter:** Investigation, Writing – review & editing. **Daniel A. Geddes:** Investigation, Writing – review & editing. **John L. Provis:** Conceptualization, Methodology, Resources, Writing – review & editing, Supervision, Project administration, Funding acquisition. **Brant Walkley:** Conceptualization, Methodology, Resources, Writing – review & editing, Supervision, Project administration, Funding acquisition.

## Declaration of Competing Interest

The authors declare the following financial interests/personal relationships which may be considered as potential competing interests: Brant Walkley reports financial support was provided by UKRI Innovate UK, EPSRC and Lubrizol Ltd. John L. Provis reports financial support was provided by UKRI Innovate UK, EPSRC and Lubrizol Ltd.

## Acknowledgement

The authors are grateful to UKRI Innovate UK, EPSRC and Lubrizol Ltd. for funding through a Knowledge Transfer Partnership (Ref: 12041). The authors are also thankful to Dr Andrew Fairburn and Dr Linden Drezet, Department of Civil Engineering, The University of Sheffield, for assistance with running the TOC measurements, and Dr Esther Karunakaran, Department of Chemical and Biological Engineering, The University of Sheffield, for the use of the ZetaPALS instrument.

## References

[1] J.L. Provis, S.A. Bernal, Geopolymers and related alkali-activated materials, Annu. Rev. Mater. Res. 44 (2014) 299–327.
[2] K. Arbi et al., A review on the durability of alkali-activated fly ash/slag systems: advances, issues, and perspectives, Ind. Eng. Chem. Res. 55 (19) (2016) 5439–5453.
[3] J.S.J. van Deventer et al., Chemical research and climate change as drivers in the commercial adoption of alkali activated materials, Waste Biomass Valorization 1 (1) (2010) 145–155.
[4] J.L. Provis, J.S.J. van Deventer, Alkali activated materials: state-of-the-art report, RILEM TC 224-AAM, Springer Science & Business Media, 2014.
[5] P. Duxson, J.L. Provis, Designing precursors for geopolymer cements, J. Am. Ceram. Soc. 91 (12) (2008) 3864–3869.
[6] P.-C. Aïtcin, R.J. Flatt, Science and technology of concrete admixtures, Woodhead Publishing, 2015.
[7] P.K. Mehta, P.J. Monteiro, Concrete microstructure, properties and materials, 4th ed., McGraw-Hill, 2017.
[8] M. Palacios, F. Puertas, Stability of superplasticizer and shrinkage-reducing admixtures Stability of superplasticizer and shrinkage-reducing admixtures in high basic media, Materiales de Construcción 54 (276) (2004) 65–86.
[9] J.Y. Yoon, J.H. Kim, Evaluation on the consumption and performance of polycarboxylates in cement-based materials, Constr. Build. Mater. 158 (2018) 423–431.
[10] M. Palacios et al., Adsorption of superplasticizer admixtures on alkali-activated slag pastes, Cem. Concr. Res. 39 (8) (2009) 670–677.
[11] B. Nematollahi, J. Sanjayan, Effect of different superplasticizers and activator combinations on workability and strength of fly ash based geopolymer, Mater. Des. 57 (2014) 667–672.
[12] A. Kraus, et al., Cationic copolymers, 2016. https://patents.google.com/patent/US20160369024A1/en
[13] C. Wang, O. Kayali, J.-L. Liow, Effect of electrostatic repulsion induced by superplasticizers on the flow behaviour of fly ash pastes, in: Fifth International Conference on Sustainable Construction Materials and Technologies, London, UK, 2019.
[14] M. Ilg, J. Plank, Non-adsorbing small molecules as auxiliary dispersants for polycarboxylate superplasticizers, Colloids Surf., A 587 (2020) 124307.

[15] M.H. Derkani et al., Mechanisms of surface charge modification of carbonates in aqueous electrolyte solutions, Colloids Interfaces 3 (4) (2019) 62.
[16] R.J. Hunter, Zeta potential in colloid science: principles and applications, vol. 2, Academic Press, 2013.
[17] M. Lesti, S. Ng, J. Plank, $Ca^{2+}$-mediated interaction between microsilica and polycarboxylate comb polymers in a model cement pore solution, J. Am. Ceram. Soc. 93 (10) (2010) 3493–3498.
[18] C. Schröfl, M. Gruber, J. Plank, Preferential adsorption of polycarboxylate superplasticizers on cement and silica fume in ultra-high performance concrete (UHPC), Cem. Concr. Res. 42 (11) (2012) 1401–1408.
[19] C.-Z. Li, N.-Q. Feng, R.-J. Chen, Effects of polyethlene oxide chains on the performance of polycarboxylate-type water-reducers, Cem. Concr. Res. 35 (5) (2005) 867–873.
[20] A. Habbaba, J. Plank, Surface chemistry of ground granulated blast furnace slag in cement pore solution and its impact on the effectiveness of polycarboxylate superplasticizers, J. Am. Ceram. Soc. 95 (2) (2012) 768–775.
[21] J. Plank et al., Effectiveness of polycarboxylate superplasticizers in ultra-high strength concrete: the importance of PCE compatibility with silica fume, J. Adv. Concr. Technol. 7 (1) (2009) 5–12.
[22] M. Schmid, J. Plank, Dispersing performance of different kinds of polycarboxylate (PCE) superplasticizers in cement blended with a calcined clay, Constr. Build. Mater. 258 (2020) 119576.
[23] R. Li et al., Effectiveness of PCE superplasticizers in calcined clay blended cements, Cem. Concr. Res. 141 (2021) 106334.
[24] J.O. Malta et al., Characterization and stabilization of nano-metakaolin colloidal suspensions, Powder Technol. 383 (2021) 43–55.
[25] F. Pacheco-Torgal et al., Composition, strength and workability of alkali-activated metakaolin based mortars, Constr. Build. Mater. 25 (9) (2011) 3732–3745.
[26] T. Bakharev, J.G. Sanjayan, Y.-B. Cheng, Effect of admixtures on properties of alkali-activated slag concrete, Cem. Concr. Res. 30 (9) (2000) 1367–1374.
[27] C. Bilim et al., Influence of admixtures on the properties of alkali-activated slag mortars subjected to different curing conditions, Mater. Des. 44 (2013) 540–547.
[28] M. Palacios, P.F. Banfill, F. Puertas, Rheology and setting of alkali-activated slag pastes and mortars: Effect of organic admixture, ACI Mater. J. 105 (2) (2008) 140.
[29] M. Palacios, F. Puertas, Effect of superplasticizer and shrinkage-reducing admixtures on alkali-activated slag pastes and mortars, Cem. Concr. Res. 35 (7) (2005) 1358–1367.
[30] M. Palacios, F. Puertas, Effect of shrinkage-reducing admixtures on the properties of alkali-activated slag mortars and pastes, Cem. Concr. Res. 37 (5) (2007) 691–702.
[31] M. Criado et al., Alkali activated fly ash: effect of admixtures on paste rheology, Rheol. Acta 48 (4) (2009) 447–455.
[32] D.L. Kong, J.G. Sanjayan, Effect of elevated temperatures on geopolymer paste, mortar and concrete, Cem. Concr. Res. 40 (2) (2010) 334–339.
[33] A.I. Laskar, R. Bhattacharjee, Effect of plasticizer and superplasticizer on rheology of fly-ash-based geopolymer concrete, ACI Mater. J. 110 (5) (2013) 513–518.
[34] F. Puertas et al., Effect of superplasticisers on the behaviour and properties of alkaline cements, Adv. Cem. Res. 15 (1) (2003) 23–28.
[35] A.M. Rashad, A comprehensive overview about the influence of different admixtures and additives on the properties of alkali-activated fly ash, Mater. Des. 53 (2014) 1005–1025.
[36] J. Xie, O. Kayali, Effect of superplasticiser on workability enhancement of Class F and Class C fly ash-based geopolymers, Constr. Build. Mater. 122 (2016) 36–42.
[37] J.G. Jang, N. Lee, H.-K. Lee, Fresh and hardened properties of alkali-activated fly ash/slag pastes with superplasticizers, Constr. Build. Mater. 50 (2014) 169–176.
[38] I. Mithanthaya et al., Influence of superplasticizer on the properties of geopolymer concrete using industrial wastes, Mater. Today:. Proc. 4 (9) (2017) 9803–9806.
[39] R.A. Lauten, Comparison of three plasticizers in carbonate-activated slag concrete, ACI Special Publication, 2017. 320: p. 26.1-26.10.
[40] A.B. Malkawi et al., Effect of plasticizers and water on properties of HCFA geopolymers, Key Eng. Mater. 733 (2017) 76–79.
[41] S.M. Laskar, S. Talukdar, Preparation and tests for workability, compressive and bond strength of ultra-fine slag based geopolymer as concrete repairing agent, Constr. Build. Mater. 154 (2017) 176–190.
[42] L. Lei, H.-K. Chan, Investigation into the molecular design and plasticizing effectiveness of HPEG-based polycarboxylate superplasticizers in alkali-activated slag, Cem. Concr. Res. 136 (2020) 106150.
[43] T. Su, Y. Zhou, Q. Wang, Recent advances in chemical admixtures for improving the workability of alkali-activated slag-based material systems, Constr. Build. Mater. 272 (2021) 121647.
[44] M. Palacios, C. Sierra, F. Puertas, Techniques and methods of characterization of admixtures for the concrete, Materiales de Construcción 53 (269) (2003) 89–105.
[45] S.H. Bong et al., Efficiency of different superplasticizers and retarders on properties of 'one-part' fly ash-slag blended geopolymers with different activators, Materials 12 (20) (2019) 3410.
[46] B. Nematollahi, J. Sanjayan, Efficacy of available superplasticizers on geopolymers, Res. J. Appl. Sci., Eng. Technol. 7 (7) (2014) 1278–1282.
[47] F. Puertas et al., Alkali-activated slag concrete: Fresh and hardened behaviour, Cem. Concr. Compos. 85 (2018) 22–31.
[48] T. Luukkonen et al., Suitability of commercial superplasticizers for one-part alkali-activated blast-furnace slag mortar, J. Sustain. Cem.-Based Mater. 8 (4) (2019) 244–257.
[49] Y. Alrefaei, Y.-S. Wang, J.-G. Dai, The effectiveness of different superplasticizers in ambient cured one-part alkali activated pastes, Cem. Concr. Compos. 97 (2019) 166–174.
[50] L. Wang et al., The role of zinc in metakaolin-based geopolymers, Cem. Concr. Res. 136 (2020) 106194.
[51] J.C. Thomas et al., Observation of field-dependent electrophoretic mobility with phase analysis light scattering (PALS), Langmuir 18 (11) (2002) 4243–4247.
[52] F. McNeil-Watson, W. Tscharnuter, J. Miller, A new instrument for the measurement of very small electrophoretic mobilities using phase analysis light scattering (PALS), Colloids Surf., A 140 (1–3) (1998) 53–57.
[53] B. Walkley et al., Reversible adsorption of polycarboxylates on silica fume in high pH, high Ionic strength environments for control of concrete fluidity, Langmuir 38 (5) (2022) 1662–1671.
[54] H. Geng et al., Effect of pre-dispersing metakaolin in water on the properties, hydration, and metakaolin distribution in mortar, Front. Mater. 6 (2019) 99.
[55] O. Vogt et al., Reactivity and microstructure of metakaolin based geopolymers: Effect of fly ash and liquid/solid contents, Materials 12 (21) (2019) 3485.
[56] M.L. Granizo et al., Alkaline activation of metakaolin: effect of calcium hydroxide in the products of reaction, J. Am. Ceram. Soc. 85 (1) (2002) 225–231.
[57] B. Walkley, J. Provis, Solid-state nuclear magnetic resonance spectroscopy of cements, Mater. Today Adv. 1 (2019) 100007.
[58] B. Walkley et al., New structural model of hydrous sodium aluminosilicate gels and the role of charge-balancing extra-framework Al, J. Phys. Chem. C 122 (10) (2018) 5673–5685.
[59] M. El Alouani, S. Alehyen, M. El Achouri, Preparation, characterization, and application of metakaolin-based geopolymer for removal of methylene blue from aqueous solution, J. Chem. 2019 (2019) 4212901.
[60] X. Ma, M. Pawlik, Effect of alkali metal cations on adsorption of guar gum onto quartz, J. Colloid Interface Sci. 289 (1) (2005) 48–55.
[61] E. Saka, C. Guler, The effects of electrolyte concentration, ion species and pH on the zeta potential and electrokinetic charge density of montmorillonite, Clay Miner. 41 (2006) 853–861.
[62] E. Nagy, Basic equations of mass transport through a membrane layer, Elsevier, 2018.
[63] J.N. Israelachvili, Intermolecular and surface forces, Academic Press, 2011.
[64] H.-J. Butt, B. Cappella, M. Kappl, Force measurements with the atomic force microscope: Technique, interpretation and applications, Surf. Sci. Rep. 59 (1–6) (2005) 1–152.
[65] M. Manciu, E. Ruckenstein, Role of the hydration force in the stability of colloids at high ionic strengths, Langmuir 17 (22) (2001) 7061–7070.
[66] R.O. James, T.W. Healy, Adsorption of hydrolyzable metal ions at the oxide—water interface. III. A thermodynamic model of adsorption, J. Colloid Interface Sci. 40 (1) (1972) 65–81.
[67] B. Walkley et al., Incorporation of strontium and calcium in geopolymer gels, J. Hazard. Mater. 382 (2020) 121015.
[68] P. Marco, J. Llorens, Understanding of naphthalene sulfonate formaldehyde condensates as a dispersing agent to stabilise raw porcelain gres suspensions: surface adsorption and rheological behaviour, Colloids Surf., A 299 (1–3) (2007) 180–185.
[69] B.L. Mojet, S.D. Ebbesen, L. Lefferts, Light at the interface: the potential of attenuated total reflection infrared spectroscopy for understanding heterogeneous catalysis in water, Chem. Soc. Rev. 39 (12) (2010) 4643–4655.
[70] Y. Liang et al., Interaction forces between colloidal particles in liquid: Theory and experiment, Adv. Colloid Interface Sci. 134 (2007) 151–166.
[71] C. Jolicoeur, M.-A. Simard, Chemical admixture-cement interactions: phenomenology and physico-chemical concepts, Cem. Concr. Compos. 20 (2–3) (1998) 87–101.
[72] F. Dalas et al., Tailoring the anionic function and the side chains of comb-like superplasticizers to improve their adsorption, Cem. Concr. Res. 67 (2015) 21–30.
[73] L. Coppola et al., Performance and compatibility of phosphonate-based superplasticizers for concrete, Buildings 7 (3) (2017) 62.
[74] Y. He et al., Effects of polycarboxylates with different adsorption groups on the rheological properties of cement paste, J. Dispersion Sci. Technol. (2019).
[75] M.H. Derkani et al., Low salinity waterflooding in carbonate reservoirs: Review of interfacial mechanisms, Colloids Interfaces 2 (2) (2018) 20.
[76] K.S. Schmitz, Physical chemistry: Multidisciplinary applications in society, Elsevier, 2018.
[77] N. Allen et al., Calorimetric study of alkali and alkaline-earth cation adsorption and exchange at the quartz-solution interface, J. Colloid Interface Sci. 504 (2017) 538–548.
[78] R.J. Flatt, Dispersion forces in cement suspensions, Cem. Concr. Res. 34 (3) (2004) 399–408.
[79] N. Roussel et al., Steady state flow of cement suspensions: A micromechanical state of the art, Cem. Concr. Res. 40 (1) (2010) 77–84.
[80] J. Hot et al., Adsorbing polymers and viscosity of cement pastes, Cem. Concr. Res. 63 (2014) 12–19.